LOW VOLTAGE, MULTIPLE AXIS, HIGH SPEED, DROPLET MANIPULATION TECHNIQUE IN OPEN SURFACE OPTOELECTROWETTING MICROFLUIDIC DEVICE

by

Vasanth Shekar

A thesis submitted to the faculty of The University of North Carolina at Charlotte in partial fulfillment of the requirements for the degree of Master in Science in Electrical Engineering

Charlotte

2012

Approved by:

Dr.James Conrad

Dr.Srinivas Akella

Dr.Stephen Bobbio

ABSTRACT

A Lab on a Chip device scales down multiple laboratory processes to a chip capable of performing automated chemical analysis. Electrowetting on Dielectric (EWOD) is a lab on a chip technology which uses patterned electrodes for droplet manipulation. The main limitations of EWOD devices are the restriction in volume and motion of droplets due to the shape and layout of the electrodes. Optoelectrowetting on dielectric (OEWOD) device uses optical sources and electric field for droplet actuation. In this research, we report an open surface light-actuated OEWOD device which can manipulate droplets of multiple volumes ranging from 1 to 50 μL at voltage as low as 53 V_{DC}. Compared with previous open configuration devices, we added a dedicated dielectric layer (Al_2O_3) of high dielectric constant($\varepsilon_r = 9.1$) and significantly reduced the thickness of the hydrophobic layer to achieve low voltage droplet manipulation. The device is capable of transporting droplets at a maximum speed of 12 mm/sec (120 V_{DC}). The lateral electric field applied with the help of contact pads in both the vertical and horizontal axes helps us achieve multi-axis droplet movement at equal velocities. The behavioral changes in droplet actuation influenced by the optical pattern dimensions with the droplet volume is also reported.

CHAPTER 1: INTRODUCTION

Lab on a Chip (LoC) technology scales down multiple laboratory processes to a chip, capable of combining sequences to perform automated chemical analysis. *Microelectromechanical systems*(MEMS) are miniaturized versions of micro-fabricated mechanical and electro-mechanical elements. It varies from relatively simple structures having no moving elements, to extremely complex electromechanical systems with multiple moving elements. LoC devices are a subset of MEMS devices and often called as *Micro Total Analysis Systems* (μTAS).

A Lab on a Chip device can be viewed as a platform that perform functions of an organic analytical laboratory like sample pretreatment, sample transportation, mixing reaction, separation, and detection in micro volumes. A distinct benefit of miniaturized LoC systems is the dramatic (potentially thousand fold) reduction of sample consumption and increase in throughput [1].

Digital microfluidics is a multidisciplinary field which combines the knowledge of physical and chemical nature of fluids along with the micro-fabrication techniques. Digital microfluidics is applied to control and measure chemical reactions and biological processes in the micro/nano range. It also deals with the behavior, precise control, and manipulation of fluids that are geometrically constrained to a small, typically microscopic scale. The field of digital microfluidics is at the intersection of engineering, chemistry, microtechnology and biotechnology, with practical applications to micro-volume design systems. Compared to continuous flow-based techniques, digital microfluidics offers the advantage of individual sample addressing, reagent isolation and compatibility with array-based techniques.

Research exploration in digital microfluidics started in the early 1950s. In 1951,

Elmqvist reported the first practical Rayleigh break-up ink-jet device [2] by controlling and dispensing liquids (nL), revolutionizing the present ink-jet technology [3]. Terry *et al.* [4] in 1979 reported a microfluidic device which introduced microchannels in silicon wafer. Later, Shoji *et al.* [5] in 1988 implemented micro-valves in silicon wafers followed by Lintel *et al.* [6] with micro-pumps. Lintel *et al.* used silicon micromachining for micro-pumps and actuated it using piezoelectric discs.

Droplet manipulation technologies are versatile and include surface acoustic waves, thermocapillary forces, electrowetting, dielectrophoresis, and magnetic forces. Among these methods, electrowetting provides the advantage of fast response time, easy implementation, and large forces from the millimeter to micrometer scales. Electrowetting is the modification of the wetting properties of a surface with the help of external voltage. In other words, it is the electrostatic modulation of the surface tension between a solid (electrode) - liquid (droplet) interface, providing high level of control across the surface of the substrate. Microfluidic devices which work using the electrowetting principle for droplet movement are called *electrowetting on dielectric* (EWOD) devices. Figure 1.1 shows the cross-section of EWOD devices along with its layers.

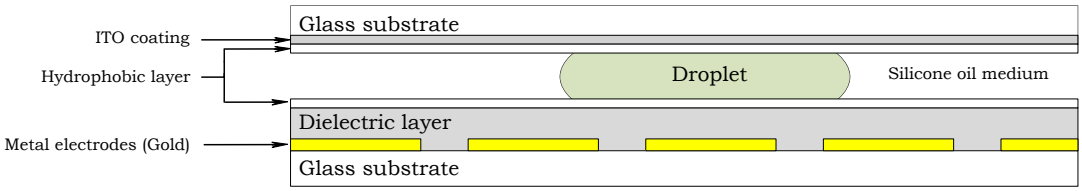

Figure 1.1: Cross-section of the EWOD device. The parallel substrates are separated by spacers and the droplet is sandwiched between the substrates.

The main limitation of the EWOD devices are the restriction in the droplet volume depending on the size of the electrode and the restriction in the droplet motion depending on the layout of electrodes. Moreover, the droplet manipulation is restricted to the regions where the electrodes are coated. To overcome these limitations, op-

tical patterns are used for droplet manipulations. The size of optical patterns can be changed depending on the droplet volume. *Optoelectrowetting* (OEW) is a light-actuated droplet manipulation technique using optical sources and electric field. The optical source generating the patterns ranges from a laser [7] to LCD screen [8]. The OEW devices are coated with a featureless photoconductive layer to eliminate the patterned electrodes. Its main advantages are the simplicity in fabrication process and large droplet manipulation region compared to EWOD devices. The devices which work using OEW for droplet manipulation are called optoelectrowetting on dielectric (OEWOD) devices.

The EWOD and OEWOD devices can be further classified into open configuration devices and closed configuration devices (Figure 1.2) based on the number of substrates used and the application of electric field. Closed configuration is a way to manipulate droplets sandwiched between two parallel substrates. The top substrate acts as a common ground, and the bottom surface is used to apply electric field. EWOD devices are generally closed configuration because it is easy to automate the process of switching voltages between the electrodes. Open configuration devices use lateral electric fields for droplet manipulation, and they have only one substrate acting as a platform for droplet manipulation. The advantage of using open configuration is because it is easy to interface the OEWOD device with other microfluidic structures such as on chip reservoirs to increase its versatility for biochemical analyses [9].

The open configuration OEWOD devices reported so far require a few kilovolt for droplet actuation [10]. It is difficult to achieve multi-axis motion in the OEWOD device because the droplet manipulation is difficult in the direction perpendicular to the applied electric field. In this research, an open configuration OEWOD microfluidic device was fabricated. The OEWOD device is capable of transporting droplets at voltages as low as 53 V_{DC}. The device is also capable of performing multi-axis droplet motion at a maximum droplet velocity of 12 mm/sec at 120 V_{DC}. The

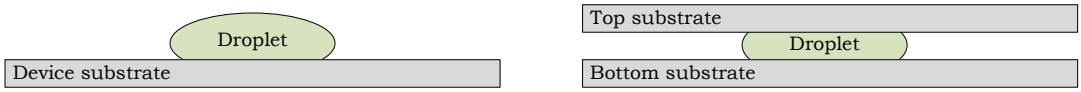

Figure 1.2: Difference between open configuration and closed configuration device. The open configuration devices have only one substrate and the external voltage is applied at the sides. The closed configuration device have a pair of substrates separated by a spacer and the droplets are sandwiched between the substrates. The external voltage is applied at the bottom substrate and the top substrate is used for connecting common ground.

significant reduction in droplet actuation voltage along with the enhanced capability of low voltage multi-axis manipulation using this OEWOD device is a step towards achieving a portable light-actuated microfluidic device.

CHAPTER 2: RELATED WORK

Electrowetting on dielectric (EWOD) devices are typically fabricated using metallic layers and photolithographic procedures [11] [12]. The metallic layer is etched to form individually addressable positions called *electrodes*. The size of an electrode defines the size or volume of droplet to be used. The electrode layer is covered with an insulating dielectric layer and hydrophobic layer. Fair *et al.* [12] explained the droplet movement mechanism and the influence of the dielectric layer in droplet motion and actuation speed.

The droplet movement is achieved by the contact angle difference at the ends of a droplet due to the voltage drop across the dielectric region. The relation between contact angle difference and the local voltage drop across the dielectric layer is given by the Young–Lippmann's equation [13] [14].

$$\cos\theta_v = \cos\theta_0 + \frac{1}{2\gamma}cV^2 \tag{2.1}$$

where θ_v is the contact angle of the droplet at applied voltage (v), and at voltage, θ_0 is the contact angle of the droplet at initial position when no voltage is applied , γ is the surface tension at the solid (device) - liquid (droplet) interface, V is the voltage drop across the dielectric layer, and c is the effective capacitance of the dielectric layer.

Wheeler *et al.* [11] reported that the EWOD device can be fabricated without using the clean rooms. They reported three different cost effective microfluidic devices fabricated using polyethylene wraps and water repellents on copper substrates. Droplet volumes from 1 to 12 μL are manipulated.

The minimum voltage required for a droplet movement is called the *threshold voltage or actuation voltage*. The threshold voltage of an EWOD device varies depending on the medium in which the droplet is manipulated. Generally the droplets are manipulated either in air medium or in an insulating oil medium (silicone oil). When compared to the air medium, the threshold voltage required for droplet manipulation is significantly lower in the oil medium [15]. The insulating oil adds lubrication to the droplet surface. As a result, the frictional force (opposing force acting on the droplet) is lower in the oil medium than in the air medium.

The threshold voltage is influenced by the dielectric layer [16]. A dielectric material is a poor conductor of electricity, but an efficient supporter of electrostatic fields [17]. The threshold voltage can be reduced by increasing the effective capacitance across the dielectric layer [13] [18]. The effective capacitance of an EWOD device can be increased by increasing the dielectric constant and decreasing the thickness of the dielectric layer. Fair *et al.* [18] fabricated multiple dielectric layers (tantalum pentoxide (Ta_2O_5), Aluminum Oxide (Al_2O_3), ParyleneC, Barium strontium titanate ((Ba,Sr)TiO_3, BST)) to increase the dielectric constant and reduced the threshold voltage as low as 6 V.

The velocity of droplet movement in an EWOD device is influenced by the external voltage applied [15]. The droplet velocity increases by increasing the applied voltage and velocities as high as 12 cm/sec are reported [19]. The maximum average velocity in EWOD device is 40 times faster than electrochemical actuation [20]. Although thermocapillary [21] and dielectrophoretic [22] methods can achieve droplet velocities equal to EWOD devices, both the methods result in substantial heating of the droplet [15].

All the above mentioned devices use patterned electrodes for droplet movement. The main limitations of the EWOD devices are:

- The volume of droplets used depend on the size of the electrode.
- The motion of the droplet depends on the layout of electrodes.
- The droplet manipulation is restricted to the regions where the electrodes are coated.

Light driven droplet manipulation can be used to overcome the limitations observed in EWOD devices. The light driven droplet manipulation can be achieved using several methods like direct optical force actuation ([23] [24]), optothermal actuation ([25] [26]), and optoelectronic actuation. Optoelectronic actuation can be subsdivided into optoelectrowetting and optoelectronic tweezers. Among these methods, optoelectrowetting (OEW) is an effective technique for its fast response, easy implementation and reliability. Devices which work using optoelectrowetting for droplet manipulation are called optoelectrowetting on dielectric (OEWOD) devices. The OEWOD devices typically works using optical source and external voltage. The device is coated with a featureless photoconductive layer followed by an insulating dielectric layer and a hydrophobic layer. Optical patterns are generated from the optical source and focused on the photoconductive layer. These optical patterns act as the electrodes for moving the droplets and can be also referred as *virtual electrodes*. The OEWOD devices are capable of transporting droplets of multiple volumes ranging from 250 pL to several μL due to the flexibility in virtual electrode dimensions. The OEW devices were first reported by Chiou *et al.* [7] who used laser beams (65 mW/cm^2) for droplet manipulation. The OEW device can perform operations like droplet injection, transportation, separation, and multi-droplet manipulation. The main limitation of the device is the presence of Indium Tin Oxide (ITO) electrodes in the device structure.

These electrodes restrict the droplet volume as observed in EWOD devices.

Chiou *et al.* [27] replaced the ITO electrodes with a featureless aluminum film. The authors used Helium Neon (HeNe) laser as the optical source for droplet volumes ranging from 10 to 50 pL and achieved droplet motion at 1 mm/sec. The device works using closed configuration model and the average velocity of droplet is very low (1 mm/sec) when compared with the EWOD devices (12 mm/sec).

Chiou *et al.* [28] reported an open surface *floating electrode optoelectronic tweezers* (FEOET) in which the aluminum film is replaced with two layers of photoconductive amorphous silicon (undoped *a-Si:H* (0.5 μm) and doped *a-Si:H* (0.1 μm). Here the authors used laser beams (4.08 μW/mm^2) and achieved a droplet motion at 85.1 μm/sec. The advantage of using open configuration model is the ability to interface and integrate other microfluidic structures such as microwells [28].

Since laser beams require expensive, difficult, and sometimes hazardous setup, Pei *et al.* [29] reported a light-actuated droplet manipulation (LADM) device in which the optical source is replaced from laser to a conventional data projector (DELL 4210X). They used a thin oxide layer (Al_2O_3) of high dielectric constant ($\varepsilon_r = 9.1$) and increased the effective capacitance of the dielectric region. The increase in effective capacitance helped in achieving droplet movement at threshold voltage as low as 16 V_{AC}. The aggressive scaling of the dielectric thickness helps to achieve high speed droplet manipulation (2 cm/sec) in low optical intensity (3 W/cm^2) [29].

Later, Chiou *et.al* [8] reported a *Single-sided continuous optoelectrowetting* (SCOEW) device which uses LCD screen for droplet actuation. The authors used a continuous photoconductive layer (0.5 μm, a-Si:H) and a thick dielectric layer (1 μm, CYTOP).

The electric field is applied at the sides of the droplet manipulation region using aluminum contact pads (0.1 μm). The authors explained that the electrowetting voltage across the capacitors in the non-illuminated sites (virtual electrode) and illuminated sites is determined by the relative ratio of photoresistances and not the absolute values. This unique property allows the optical actuation of droplets with low optical intensity. The SCOEW device is an open configuration model and the authors successfully integrated on-chip reservoirs. An on-chip reservoir can dispense droplets at specified intervals of time with less than 0.91% volume variation. The main limitation of the SCOEW device is that it requires high voltage (a few kilovolts [10]) for droplet actuation. Moreover, the droplet motion is achieved in the direction parallel to the applied electric field and it is difficult to manipulate droplets in the perpendicular direction.

In this research, an OEWOD device was fabricated that significantly improved upon the performance of the previously reported open configuration devices [10]. When compared with the most recently reported open configuration device [8], the effective capacitance of the dielectric region is increased by adding a dedicated dielectric layer (Al_2O_3, 25 nm) of high dielectric constant ($\varepsilon_r = 9.1$) and reducing the thickness of the hydrophobic layer. By increasing the effective capacitance, the threshold voltage is reduced from a few kilovolt to 53 V_{DC}. Low voltage multi-axis droplet manipulation was successfully demonstrated by enhancing the electric field strength surrounding the droplet manipulation region. The device has operated at speeds as high as 12 mm/sec and is capable of performing operations like mixing, merging, and parallel droplet manipulation.

CHAPTER 3: ELECTROWETTING ON DIELECTRIC (EWOD) DEVICE

3.1 Working Mechanism

Electrowetting is the modification of wetting property of the surface to achieve contact angle change at the droplet ends for droplet manipulation. The EWOD device consists of patterned electrodes fabricated using photolithographic process followed by the dielectric layer and hydrophobic layer. The dielectric layer/ hydrophobic layer can be modeled as capacitors. The droplet to be manipulated is introduced on top of the electrode. Electrowetting is influenced by the droplet only when a portion of the droplet overlaps the adjacent electrodes (Figure(dash)). As a result, the volume of the droplet used is based on the dimension of the patterned electrode.

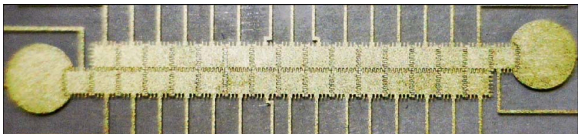

Figure 3.1: Top view of an EWOD device. The gold slots are the electrodes where the droplets are manipulated.

Figure 1.1 shows the cross-section view of an EWOD device. The electrode housing the droplet is referred as the N^{th} electrode. The adjacent electrodes are referred as $(N+1)^{th}$ and $(N-1)^{th}$ electrodes.

3.1.1 Contact angle at zero voltage

The droplet's initial contact angle will be greater than 90° due to the hydrophobic layer. When there is no voltage applied at the electrodes, there will be no contact angle change at the droplet ends and the droplet remains stationary.

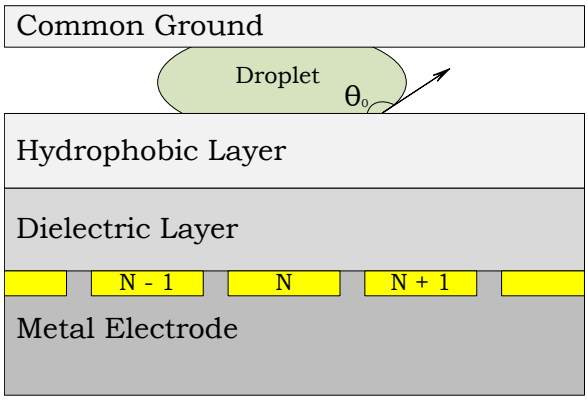

Figure 3.2: Droplet's contact angle at zero voltage. The electrode where the droplet is introduced is referred as the N^{th} electrode. The adjacent electrodes are referred as $(N+1)^{th}$ and $(N-1)^{th}$ electrodes.

3.1.2 Contact angle when external voltage is applied

When external voltage is applied at the adjacent electrode, the elctrode conducts the electric field and all the voltage drop will be across the dielectric layer. The dielectric layer/ hydrophobic layer (capacitors) induce charge (Q) buildup at the device-droplet surface expressed using Equation 4.2. The energy associated with the charge buildup (Q) is called the electrostatic energy.

$$Q = C \times V \tag{3.1}$$

As per Equation 4.2, the charge buildup increases when the voltage drop across the dielectric layer is increased and as a result the electrostatic energy increases. The force acting between the molecules of the droplet is called surface tension. The electrostatic energy reduces the surface tension of the droplet at the overlapping region of the conducting electrode ($(N+1)^{th}$ electrode) [30] [15] [13]. The relation between surface tension reduction at the droplet-device interface and the voltage drop across the dielectric layer is expressed using Lippmann's equation [30].

$$\gamma = \gamma_0 - \frac{\varepsilon}{2d}V^2 \tag{3.2}$$

where γ is the reduced surface tension of the droplet at v voltage, γ_0 is the initial surface tension of the droplet at zero voltage, ε is the dielectric constant of the dielectric layer, d is the thickness of the dielectric layer, and V is the voltage drop across the dielectric layer.

he reduction in surface tension causes improved droplet wetting at the droplet-device interface. As a result, the droplet's contact angle is reduced ($< 90°$) at the end where voltage is applied. The difference in contact angle creates a pressure gradient which leads to the bulk flow of droplet towards the conducting electrode [15].

The relation between the droplet contact angle change and the voltage drop across the dielectric layer is expressed using Young-Lippman's equation 4.4.

$$\cos\theta = \cos\theta_0 + \frac{1}{\gamma}\frac{1}{2}cV^2 \tag{3.3}$$

where θ is the contact angle of the droplet at v voltage, θ_0 is the initial contact angle of the droplet at zero voltage, c is the capacitance per unit area across the dielectric region, and V is the voltage drop across the dielectric layer.

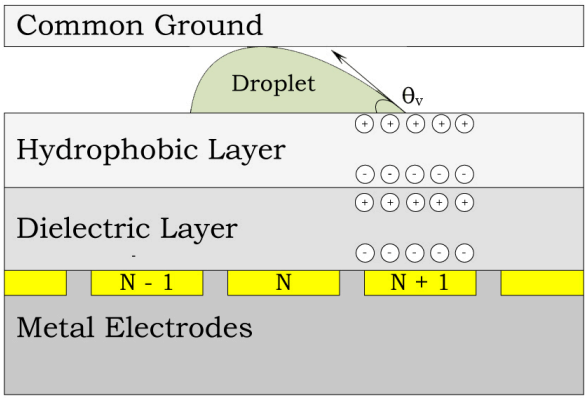

Figure 3.3: Charge build up in droplet surface. The droplet's contact angle will be reduced at the end where the external voltage is applied.

3.2 Fabrication Process

The devices are fabricated in Class 100 clean room facilities in UNCC, Charlotte and Georgia institute of technology, Atlanta. Before beginning the fabrication process, the photomask should be created to imprint the electrode layout design on the EWOD device. The region where we need the electrodes to be coated on the EWOD device will be covered by chrome in the photomask (Figure(photomask)). The photomask used for this research was designed using AutoCAD in UNCC and manufactured by *Photosciences, Inc.*

The following steps explains the clean room fabrication process of an EWOD device.

1. The substrate used are clean polished glass wafers (4" diameter) manufactured by PG&O,Inc.

2. Clean the glass substrate in piranha solution (7:3 - concentrated sulfuric acid : 30% hydrogen peroxide) for 10 minutes to remove the organic residues.

3. Coat the substrate with chromium (10 nm) and gold (100 nm) using Electron beam deposition (Lesker PVD75) as a seed layer.

4. Rinse the substrate with acetone, methanol, and DI water.

5. Bake the substrate on a hot plate at 100° C for 5 minutes.

6. Spin coat the substrate using Shipley $S1815$ photoresist at 3000 R.P.M for 30 seconds.

7. Bake the substrate on a hot plate (CEE) at 115° C for 2 minutes.

8. Expose the substrate to Ultra Violet beam (35.5 mW/cm^2, 365 nm) through the photomask using a mask aligner (Quintel) for 13 seconds.

9. Immerse substrate in MF319 developer for 60 seconds.

10. Post bake substrate on a hot plate (CEE) at 100° C for 2 minutes.

11. Immerse substrate in gold etchant for 60 seconds followed by chromium etchant for 30 seconds.

12. Rinse the substrate in DI water and post bake at 100° C for 2 minutes.

13. Coat the substrate with Al_2O_3 (50 nm) using Atomic Layer Deposition. [1].

14. Spin coat the substrate with 2 % Teflon (1:2 - 6% TeflonAF : Flourinert FC40) (250 nm) using spin coater (Laurell) at 3000 R.P.M for 60 seconds.

15. Post bake the substrate at 160° C for 10 minutes.

16. Spin coat 2 % Teflon on a separate Indium Tin Oxide (ITO) glass slide (2.5 cm $\times$ 5 cm) using spin coater (Laurell) at 3000 R.P.M for 60 seconds. This glass slide is used as the top substrate for ground connection.

17. Post bake the substrate at 160° C for 10 minutes.

Figure 3.4: Top view of a photomask

3.3 Interface electronics

Droplet manipulation in EWOD device can be automated using microcontrollers. In this research, ATMega128 microcontroller was used to automate the process. The output voltage of the microcontroller is 5 V and this voltage is not enough for manipulating the droplets. The lowest threshold voltage reported so far is 6 V and so the output voltage from the controller should be amplified before applying to the EWOD device. Relay switches are used to step-up the voltage level from 5 V to the required threshold voltage for droplet manipulation.

[1] This step is completed in Marcus Nanofabrication facility, Georgia Institute of technology, Atlanta.

A relay is an electrically operated switch used to control a circuit by a low-power signal with complete electrical isolation between control and controlled circuits (Figure(relay)). The relay circuit connections are explained in [31].

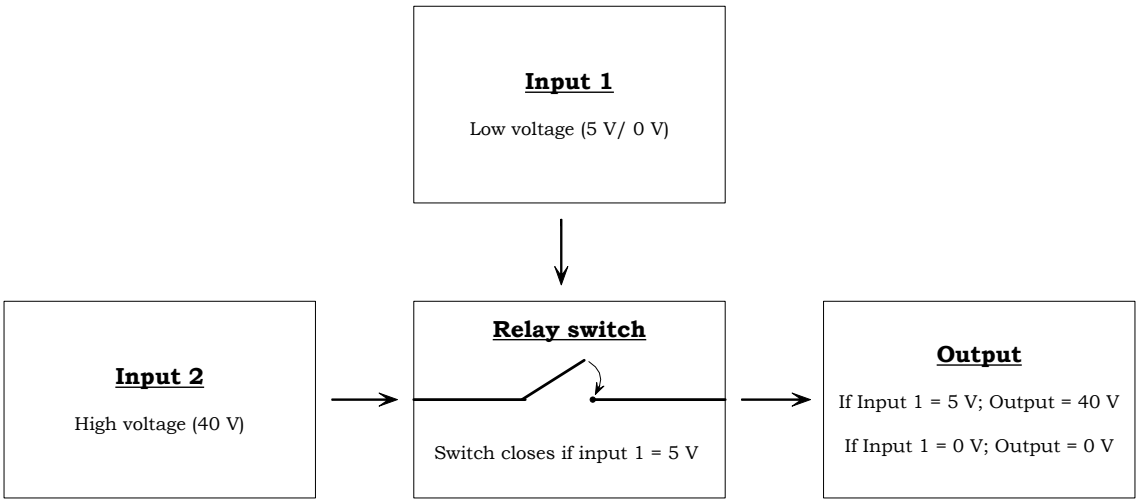

Figure 3.5: Relay switch - functional block diagram. The inputs are the low voltage signal (5 V) from the ATMega128 microcontroller and the high voltage signal from an voltage amplifier. When the low voltage signal is 5 V, then the relay switch is closed and conducts the high voltage signal to the output. When the low voltage signal is 0 V, then the relay switch is disconnected and does not conduct the high voltage signal to the output.

Since the electrodes in EWOD devices are individually addressable, each electrode should be connected with separate wires from the controller. This scenario leads to complex wiring and circuit complexities. To reduce the circuit complexities, the electrode values can be serially sent out from the microcontroller using a single port pin. The serial data from the controller can be converetd to parallel output using shift registers. A *serial in - parallel out* (SIPO) shift register can support upto 2^n (n = 1 to 5) data inputs. In this research, a 3-bit (n=3) SIPO shift register (SN74HC595N) is used which can output upto 8 electrode values as shown in the Figure(SIPO).

The SIPO shift registers and relay switches are hardwired in a printed circuit board (PCB) Figure(PCB). The input connections of the PCB are the the high voltage from the voltage amplifier and serial input from the microcontroller. The output

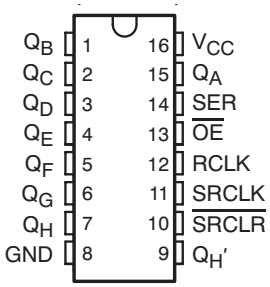

Figure 3.6: Pin configuration of serial-in/parallel-out shift register. SER (pin 14) received the serial data from the microcontroller. Q_A - Q_H are the 8 output pins (pin 1-7, pin 15) sending out the values of the microcontroller in parallel. The shift register is activated using V_{cc} (pin 16, 5 V_{DC}) and ground pin (pin 8). Pin 10 and pin 13 are the control pins which enable/disable the output values. Pin 11 is the clock signal pin where the microcontroller data is synchronized with the shift register at at clock cycles.

connections are the high voltage electrode values (ON/OFF) to be connected to the EWOD device. Figure(FBD) represents the functional block diagram showing the connections between the microcontroller, interface electronics, and the EWOD device.

3.4 Result analysis

Advancement in EWOD hardware is towards minimizing the threshold voltage [13]. By increasing the effective capacitance across the dielectric layer, we can reduce the threshold voltage required for the droplet movement [13] [18]. The effective capacitance can be increased by increasing the dielectric constant and decreasing the thickness of the dielectric layer. The influence of hydrophobic layer should also be considered in calculating the threshold voltage. The effective dielectric thickness of an EWOD device will be the sum of thicknesses of the dielectric and hydrophobic layers. Equation[5.1] explains the influence of the dielectric/hydrophobic layer with the threshold voltage [18].

$$V_{th} = D_{hy}[t_{hy} + \varepsilon_{hy}\frac{t_{di}}{\varepsilon_{di}})] \tag{3.4}$$

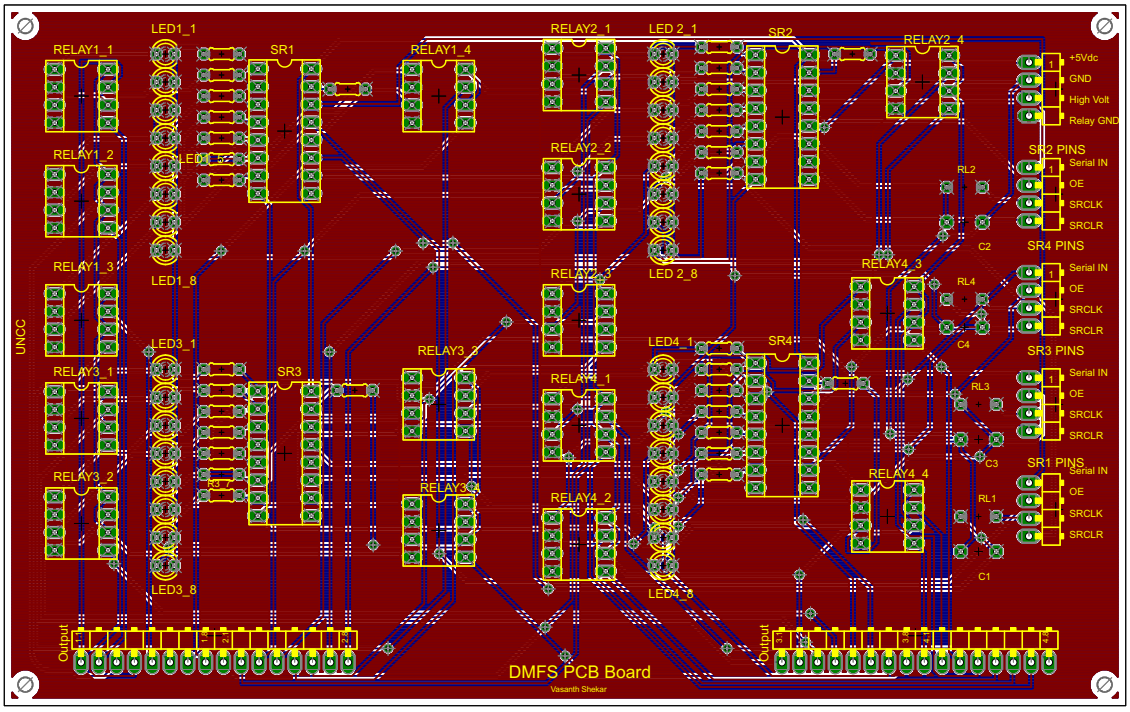

Figure 3.7: A custom-made printed circuit board is designed to assemble the shift registers and relay switches. The inputs for this PCB are the low voltage (5 V) signals from the microcontroller and the high voltage (40 V) signal from the voltage amplifier. The output is the high voltage signals from the relay switches.

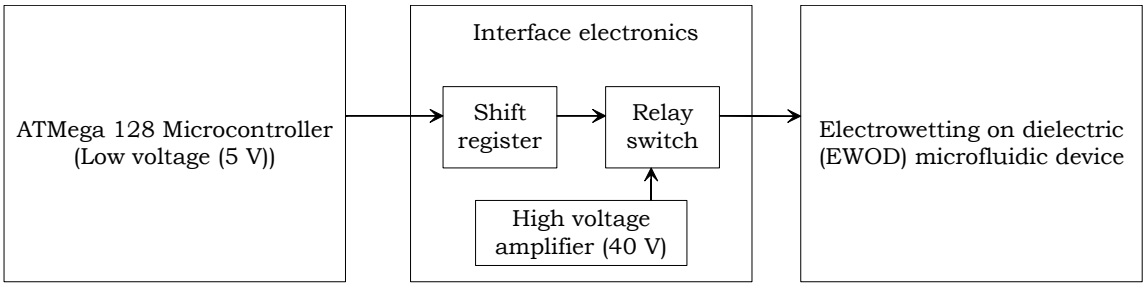

Figure 3.8: Functional block diagram of the EWOD device with the microcontroller and interface electronics. The low voltage from the output ports of the microcontroller is connected to the shift register followed by voltage step-up through relay switches. The high voltage output from the relay switches are connected to the EWOD electrodes.

The equation suggests that the threshold voltage decreases when the dielectric constant (ε_{di}) of the dielectric layer is increased and increases when the thickness of

hydrophobic layer (t_{hy}) is increased. Hence by reducing t_{hy} and increasing ε_{di}, we can effectively reduce the threshold voltage.

To verify the analysis, two sets of EWOD devices are fabrciated using similar fabrication process, but different dielectric materials and dielectric layer thicknesses are coated for each device.

CASE 1: The first set of EWOD devices (D_p) are coated with a *ParyleneC* as dielectric layer (1 μm). ParyleneC is a polymer compound ($\varepsilon_r = 3.15$) coated using Parylene coater.

CASE 2: The second set of EWOD devices (D_a) are coated with *Aluminum oxide* *(Al_2O_3)* as dielectric layer (25 nm). Aluminum oxide is an amphoteric metal oxide ($\varepsilon_r = 9.1$) coated using Atomic Layer Deposition (ALD).

Both the devices have the same teflon thickness (250 nm). The effective capacitance of the EWOD device can be expressed using Equation 3.5.

$$C_{effective} = \varepsilon_0 A[\frac{\varepsilon_d \varepsilon_h}{(\varepsilon_d t_h) + (\varepsilon_h t_d)}] \tag{3.5}$$

$C_{effective}$ is the effective capacitance of the device, ε_0 is the vacuum permittivity, A is the area of the capacitor parallel plates, ε_d and ε_h are the dielectric constants of dielectric and hydrophobic layers, and t_d and t_h are the thicknesses of dielectric and hydrophobic layers.

Using Equation[3.5], the effective capacitance of the both the devices are calculated and D_a has higher capacitance than D_p. Similarly, the threshold voltage is calculated using Equation[5.1] by substituting the values of t_{hy}, ε_{hy}, t_{di}, ε_{di} and the calculated results show that the threshold voltage of device D_a is six times less than the D_p .

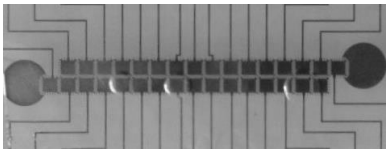

(a)

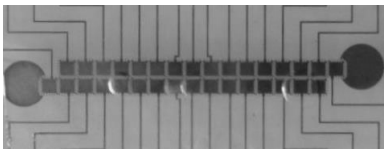

(b)

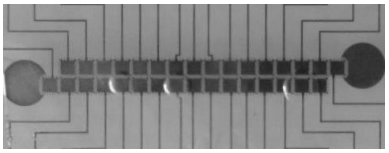

(c)

Figure 3.9: Sequence of droplet movement in EWOD device. The device is coated with Al_2O_3 as dielectric layer. Each figure is separated by a time interval of 0.033 *seconds*. (a) The droplet's initial position (b) Voltage is applied at the droplet's adjacent electrode (right side of the droplet) and the droplet starts moving towards it. (c) Droplet reached the destination electrode.

Table 3.1: EWOD

Parameters	**Device D_p**	**Device D_a**
Dielectric material	ParyleneC	Al_2O_3
Dielectric layer thickness	1000 nm	50 nm
Dielectric constant	3.15	9.1
Threshold Voltage (Calculated result)	281.03 V	54.81 V
Threshold Voltage (Experimental result)	273.5 V	40.5 V

3.4.1 Experiment analysis

Experiments are conducted on both the devices (D_p and D_a) to verify the observations in threshold voltage reduction. Table **??** explains the threshold voltages of the both devices. The following figures show the sequence of droplet movements in the EWOD device (Al_2O_3 as dielectric layer).

The distance traveled by the droplet from its initial position to final position is around 1.94 mm (calculated using the AUTOCAD measurement tools). The time taken for the droplet to reach that distance is around 167 ms (calculated using Adobe after effects). The speed of the droplet movement is calculated and it is approximately

1.2 cm/sec.

3.4.2 Inference

The threshold voltage required for a droplet movement can be reduced by increasing the effective capacitance of the device. The effective capacitance can be increased by increasing the effective dielectric constant and reducing the overall dielectric thickness of the device.

CHAPTER 4: OPTOELECTROWETTING ON DIELECTRIC (OEWOD) DEVICE

4.1 Introduction

Electrowetting is one of the most effective methods of droplet manipulation for its low electrical power consumption, easy implementation, and fast response. Electrowetting on Dielectric devices (EWOD) use patterned electrodes for droplet manipulation. *Optoelectrowetting* (OEW) is a light actuated droplet manipulation technique using optical animation patterns and external voltage. The optical source for generating the patterns can be from a laser [7] to an LCD screen [8]. The devices are coated with a featureless photoconductive layer to eliminate the patterned electrodes. A dielectric layer is deposited over the photosensitive material to provide electrical insulation. The hydrophobic layer is coated as the top surface to avoid the droplet contamination with the device surface. The device which uses optoelectrowetting principle for droplet manipulation is called optoelectrowetting on dielectric (OEWOD) device. The droplets are manipulated by illuminating the photoconductive layer with optical patterns and external voltage. Since the optical patterns are driving the droplet, it can be also referred as *virtual electrodes*. The region where the droplets can be manipulated in the device is called the active region and the remaining regions are coated with contact pads (opaque) for applying lateral electric field. The main advantages of the OEWOD devices are the elimination of photolithographic process, flexibility in changing the droplet volume at any given time and large droplet manipulation region.

4.2 Fabrication Process

Figure 4.1 shows the top view representation of the fabricated OEWOD device. The device is made up of a plain polished glass substrate (1 mm thick, 100 mm diameter).

1. The substrate is cleaned using piranha solution (7:3 - concentrated sulfuric acid : 30% hydrogen peroxide) for 10 minutes to remove the organic residues.

2. A photoconductive film of hydrogenated amorphous silicon (a-Si:H) layer is deposited (0.5 μm) using Plasma Enhanced Chemical Vapor Deposition (PECVD).[1]

3. The contact pads are coated with gold (100 nm) and chromium (10 nm) using Electron beam deposition (LESKER PVD75). An aluminum foil is used as a pattern mask to protect the active region from metal deposition.

4. A thin, pin-hole free film of dielectric aluminum oxide (Al_2O_3) (25 nm) is deposited using Atomic layer deposition (ALD). [2]

5. The substrate is spin coated with 2 % Teflon (1:2 - 6% TeflonAF : Flourinert FC40) (250 nm) using spin coater (Laurell) at 3000 R.P.M for 60 seconds.

6. The substrate is post baked at 160° C for 10 minutes.

4.3 Working Principle

Figure 4.2 shows the equivalent circuit model of the OEWOD device. The photoconductive layer (a-Si:H) is modeled as resistances R_1, R_2, R_3, R_4 connected in series. The dielectric layer is modeled as capacitors C_{d1}, C_{d2}, C_{d3} forming a shunt circuit with the resistances. The hydrophobic material (TeflonAF) also have dielectric properties

[1]This process is completed by sending the substrates to Noel Technologies, Inc.

[2]This step is fabricated in Marcus nano-fabrication facility in Georgia Institute of Technology, Atlanta, GA.

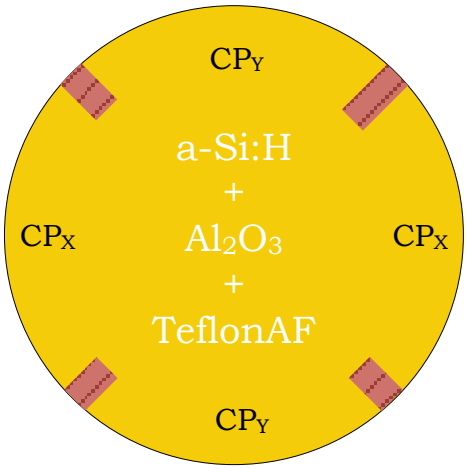

Figure 4.1: Optoelectrowetting on dielectric (OEWOD) device - Top view. The droplet manipulation region (shaded) consists of a photoconductive layer (a-Si:H), dielectric layer (Al_2O_3), and hydrophobic layer (2 % TeflonAF). CP_x and CP_y are the contact pads used for applying external voltage. The voltage is applied at CP_x, when the droplets are moving along X axis and the voltage is applied at CP_y, when the droplets are moving along Y axis

and it can also be modeled as capacitors C_{h1}, C_{h2}, C_{h3} connected in series with C_{d1}, C_{d2}, C_{d3} respectively. The effective capacitance C_1 will be equal to C_{h1} in series with C_{d1} and it can be expressed using Equation[4.1].

$$C_1 = \varepsilon_0 A[\frac{\varepsilon_{d1}\varepsilon_{h1}}{(\varepsilon_{d1}t_{h1}) + (\varepsilon_{h1}t_{d1})}] \tag{4.1}$$

ε_0 is the vacuum permittivity, A is the area of the capacitor parallel plates. The effective capacitances C_2 and C_3 are similarly expressed using C_{d2} - C_{h2} and C_{d3} - C_{h3}

When the droplets are introduced on the device, it tries to repel the surface due to the hydrophobic layer. In this case the droplet's contact angle with the surface is greater than 90° (Figure 4.2).

4.3.1 Symmetrical illumination

When the device is uniformly illuminated by dark light or bright light, the applied voltage linearly drops between R_1 to R_4. As a result, the voltage drop across

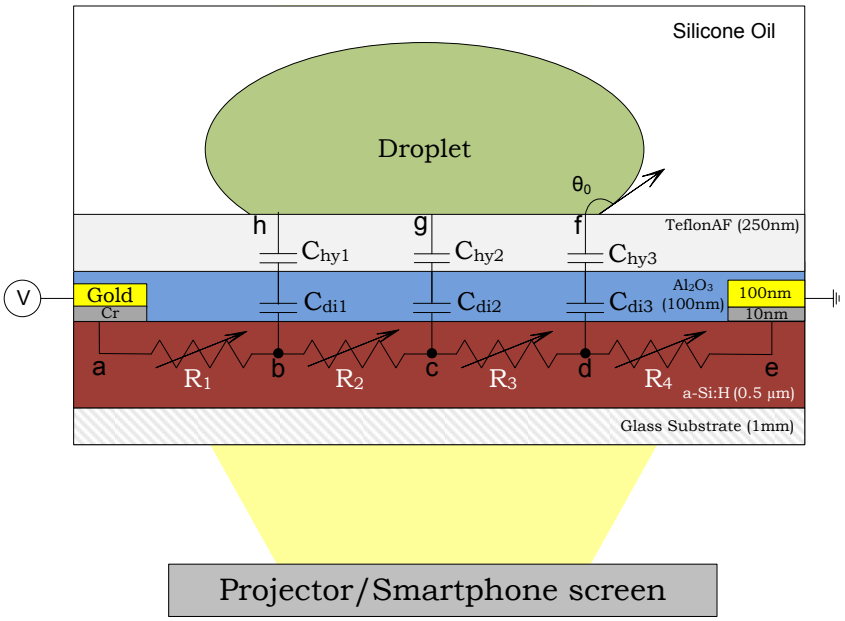

Figure 4.2: Equivalent Circuit of open surface optoelectrowetting dielectric (OEWOD) device.

capacitors C_1 and C_3 will be equal and the droplet will not have any contact angle change (Figure 4.3).

4.3.2 Asymmetrical illumination

When a portion of droplet is illuminated by bright light and the remaining region by dark light (virtual electrode) (Figure 4.4), the photoresistances R_1, R_2, and R_4 carries low resistance due to bright illumination whereas R_3 carries high resistance due to dark illumination. As a result, the voltage drop across the capacitors C_1 and C_2 will be low due to low voltage drop across R_1 and R_2 respectively. Subsequently, the voltage drop across C_3 will be high due to high voltage drop across R_3. When there is an voltage drop across the capacitor, it induces charges (Q) buildup and expressed by Equation 4.2.

$$Q = C \times V \tag{4.2}$$

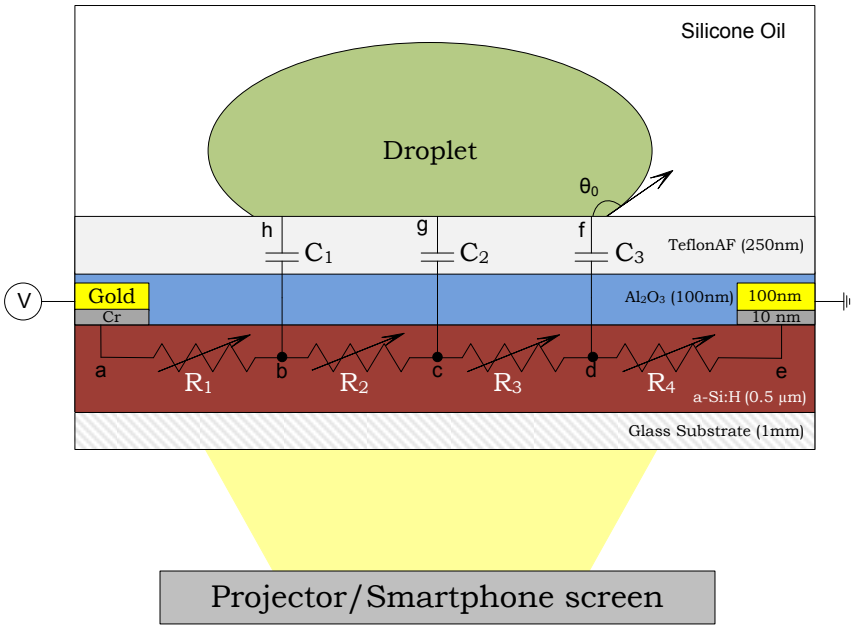

Figure 4.3: Equivalent circuit of open surface optoelectrowetting on dielectric (OEWOD) device.

Q is the charge buildup at the device-droplet interface, C is the effective capacitance of the device, and V is the voltage drop across the dielectric region.

Q_1, Q_2, and Q_3 are the charge build up across C_1, C_2, and C_3 respectively. According to Equation[4.2], the value of Q_3 will be higher than Q_1 and Q_2 because the voltage drop across C_3 is higher than C_1 and C_2.

The energy associated with the accumulated charges is called the electrostatic energy. The force acting between the molecules of the droplet is called the surface tension. The electrostatic energy acts as an opposing force and reduces the surface tension of the droplet at the solid-liquid interface [13] [15]. As a result, the surface tension is reduced at one end of the droplet and remains the same at the other end. The reduction in surface tension due to electrostatic force is given by Lippmann's equation [14].

$$\gamma = \gamma_0 - \frac{\varepsilon}{2d}V^2 \tag{4.3}$$

where γ is the reduced surface tension of the droplet at v voltage, γ_0 is the initial surface tension of the droplet at zero voltage, ε is the dielectric constant of the dielectric layer, d is the thickness of the dielectric layer, and V is the voltage drop across the dielectric layer.

The reduction of surface tension causes improved droplet wetting at the droplet end near C_3. Now, the contact angle of the droplet end near C_3 is lower than the contact angle of the droplet near C_1 (Figure 4.4). The relation between the droplet contact angle change and the voltage drop across the dielectric layer is given by Young Lippmann's Equation.

$$\cos\theta = \cos\theta_0 + \frac{1}{\gamma}\frac{1}{2}cV^2 \tag{4.4}$$

where θ is the contact angle of the droplet at v voltage, θ_0 is the initial contact angle of the droplet at zero voltage, c is the capacitance per unit area across the dielectric region, and V is the voltage drop across the dielectric layer.

The difference in contact angle creates a pressure gradient, which leads to the bulk flow of the droplet towards the non-illuminated region (virtual electrode) [15] [8].

4.4 Laboratory setup

Figure 4.5 shows the experimental setup for droplet actuation in OEWOD device. Initially the device is immersed in a silicone oil medium is kept inside a transparent petri dish. The following equipment are used for manipulating droplets in the OEWOD device.

- Commercial data projector (Dell 4210X) is used as the optical source and the projector is controlled using a personal computer.
- Wooden stand is used for placing the OEWOD device setup on top of the optical source (Figure 4.5).

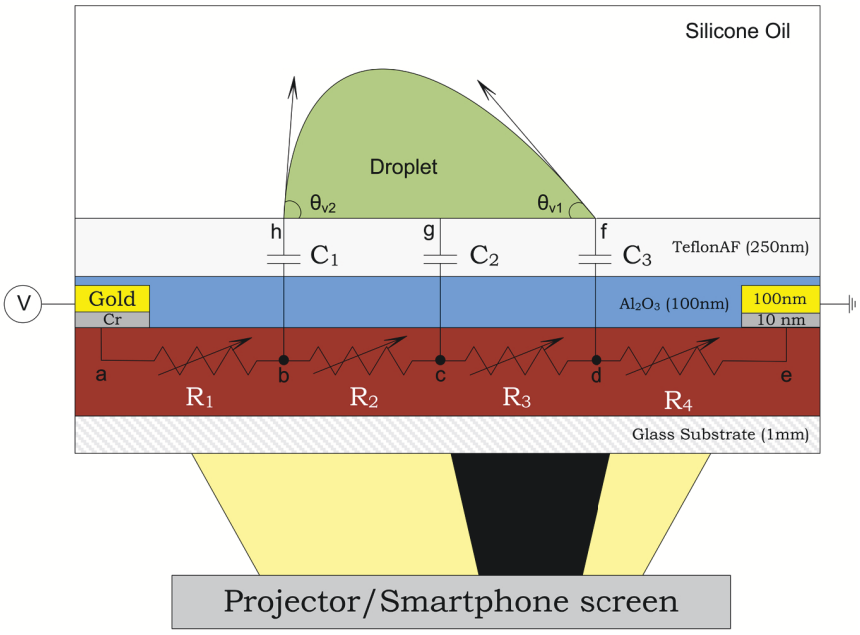

Figure 4.4: Circuit behavior when there is a bright illumination in one end of the droplet (region under R_1, R_2, and R_4) and dark illumination in the other end of the droplet (region under R_3). R_1, R_2, and R_4 carries low resistance due to bright illumination and R_3 carries high resistance due to dark illumination.

- A Dinolite (D413T) microscopic camera placed directly on top of the device for recording the droplet movements.
- The external voltage is applied using Trek 2205 voltage amplifier which is powered by EZ 4303D adjustable DC power supply.
- The droplets are introduced to the OEWOD device using microliter syringe from Hamilton company, Inc.

4.4.1 Optical pattern generation

The optical patterns are generated using a canvas enabled JavaScript application. Canvas features of JavaScript will run in any modern internet browsing user agent with or without internet connection. The JavaScript application is highly portable and quickly adaptable on wide range of devices including desktop connected to a monitor or a projector, smart phones (Iphone), or a touchscreen tablet device (Ipad).

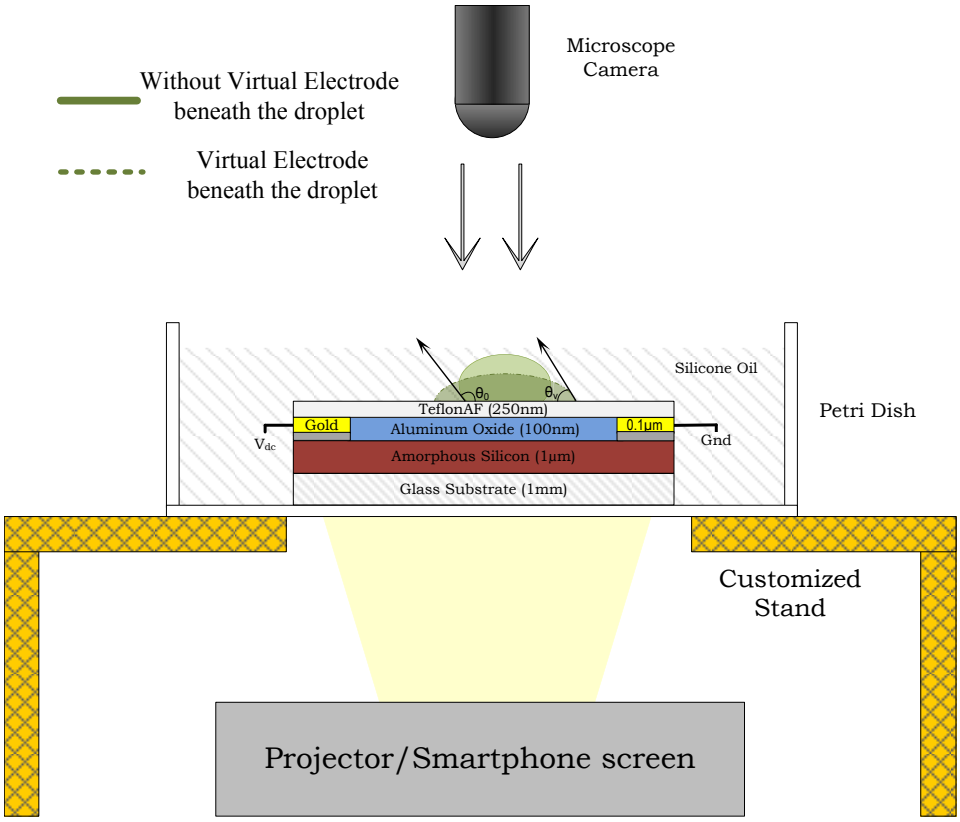

Figure 4.5: Side view of the OEWOD device laboratory setup. The OEWOD device is immersed in silicone oil stored in the petri dish. The camera is stationed on top of the OEWOD device to record the droplet movement.

Features of the OEWOD animation

In this research, the optical patterns are controlled using mouse clicks and keyboard commands. The optical interface has two main components - Settings menu and an animation canvas. The settings menu is the control end of the animation file where the size, shape, position, movement velocity, and the color of the optical patterns are adjusted (represented in pixels)(Figure: animation canvas). The animation canvas is the region where the optical patterns are drawn. (Figure see fig:droplet controls).

CHAPTER 5: RESULT

5.1 Experimental Results and Analysis

The fabricated OEWOD device is capable of performing operations like droplet transportation, merging, multi-axis movement, parallel manipulation, and different volume droplet manipulation.

5.1.1 Experiment Procedure

Initially the device is immersed in a silicone oil medium (for lubrication) stored in a transparent petri dish. The droplets are then introduced on the active region of the device surface. The active region is the area where droplets can be manipulated using optical patterns. The remaining regions are covered with gold contact pads (opaque) where manipulation is not possible. The droplet manipulation region is illuminated by animation patterns from a data projector (DELL 4210X) (Figure 5.1). The external voltage is applied in the contact pad sets (CP_1 or CP_2) shown in Figure 5.2. The droplets are driven by rectangular dark light and the remaining active region is filled with bright white light as shown in Figure 5.3.

5.1.2 Reduction in Threshold Voltage

Advancement in digital microfluidics in recent years is going towards achieving a portable microfluidic device [10]. Reduction in threshold voltage is a key parameter in achieving this goal since it eliminates bulky voltage amplifiers. By actuating droplets in low input voltage, we can use lithium batteries as an input voltage source to achieve device portability.

To reduce the threshold voltage (V_{th}) from previously reported devices, a designated

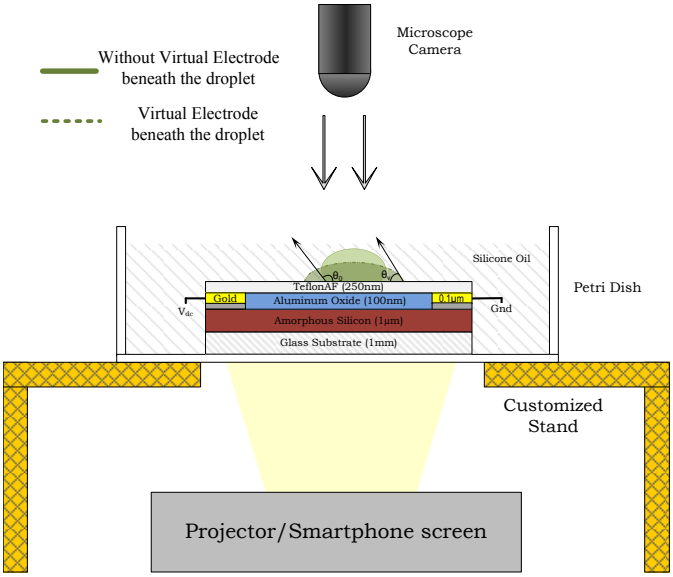

Figure 5.1: Side view of the OEWOD microfluidic device inside the petri dish. The optical illumination from the data projector light is focused on the device from below.

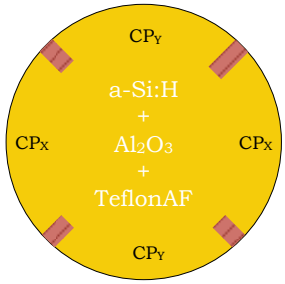

Figure 5.2: Top view representation of the OEWOD device. The dark red shaded region is the droplet manipulation region. CP_1 and CP_2 are the contact pad sets (yellow region) where the external voltage is applied.

dielectric layer (Al_2O_3) of high dielectric constant ($\varepsilon_r = 9.1$) is included in the fabrication process. High dielectric constant materials can also increase the net force on the droplet [32] thereby increasing the droplet velocity. By including Al_2O_3 in the fabrication process we successfully reduced the threshold voltage from a few kilo volts [10] to 53 V_{DC}. To experimentally analyze the significance of the dielectric layer, we fabricated two sets of devices with different thicknesses of Al_2O_3. The first set of devices (Device D_{10}) are coated with 500 nm a-Si:H, 100 nm gold contact pads, 10

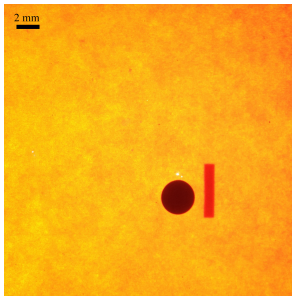

Figure 5.3: Top view of the OEWOD device active region. The droplet can be manipulated anywhere in the active region the virtual electrode (dark rectangle next to the droplet).

Table 5.1: Performance comparison in device D_{10} and device D_{25}.

Parameters	**Device** D_{10}	**Device** D_{25}
Dielectric layer thickness	10 nm	25 nm
Threshold Voltage (calculated result)	54.2 V_{DC}	52.8 V_{DC}
Threshold Voltage (Experimental result)	68 V_{DC}	53 V_{DC}
Average Velocity	3.5 mm/sec	8 mm/sec

nm Al_2O_3, and 250 nm 2% TeflonAF. The second set of devices (Device D_{25}) are coated with similar process as in (Device D_{10}) except the thickness of Al_2O_3 (25nm). The optical source is the same for both the devices (1.069 mW/cm^2).

The results are tabulated (Table 5.1). Device D_{25} shows improved performance over device D_{10} in terms of threshold voltage. Using Equation 5.1 given in [18], we calculated the threshold voltage by substituting the values of t_{hy}, ε_{hy}, t_{di}, ε_{di}.

$$V_{th} = D_{hy}[t_{hy} + \varepsilon_{hy}\frac{t_{di}}{\varepsilon_{di}})] \tag{5.1}$$

where V_{th} is the threshold voltage for the device, D_{hy} is the dielectric strength of hydrophobic material used, t_{hy} and t_{di} are the thicknesses of the hydrophobic and dielectric layers, ε_{hy} and ε_{di} are the dielectric constants of hydrophobic and dielectric layers respectively.

The equation suggests that the threshold voltage decreases when the dielectric

constant (ε_{di}) of the dielectric layer is increased and increases when the thickness of hydrophobic layer (t_{hy}) is increased. Hence by reducing t_{hy} and increasing ε_{di}, we can effectively reduce the threshold voltage and Table 5.1 verified this analysis.

5.1.3 High speed droplet manipulation

The fabricated OEWOD device (device D_{25}) is capable of transporting droplets at a maximum speed of 12 mm/sec (120 V_{DC}). Device D_{25} shows improved performance in average droplet velocity when compared to device. The effective capacitance in device D_{25} is higher than device D_{10} due to the thicker dielectric layer in device D_{25}. The net force acting on the droplet is proportional to the capacitative energy per unit area stored in the dielectric layer [29]. As a result, the net force acting on the droplet in device D_{25} is higher than device D_{10} and hence the average droplet velocity is higher in device D_{25} than device D_{10}. In general, we can say that the droplet velocity is higher in devices with higher effective capacitance across the dielectric layer.

$$F_{net} \simeq \frac{\varepsilon}{D} V^2 \tag{5.2}$$

where F_{net} is the net force acting on the droplet, ε is the effective dielectric constant across the device, D is the cumulative distance of the dielectric layers in the device, and V is the voltage drop across the dielectric layers.

5.1.4 Variation in contact angle by optoelectrowetting

The following cases occur when voltage V is applied to the microfluidic device.

Case one: When there is a uniform illumination (bright light) under the droplet, the contact angle remains the same at both the droplet ends (Figure 5.4(a)) and it is approximately 150°.

Case two: When the region under the droplet is illuminated by dark light and the remaining region by white light, the contact angle is reduced at both the ends but

remains the same due to equal illumination at droplet ends. Figure 5.4(b) shows the contact angle reduced at both the droplet and it is approximately 120°.

Case three: When a portion of the droplet is illuminated by the dark light and the remaining region by white light, the droplet's contact angle is reduced in the dark region due to thus creating a contact angle difference ($\Delta\theta$)(Figure 5.4(c)) shows the contact angles at ends of the droplet (125° and 85°) and the measured $\Delta\theta$ is approximately 40°.

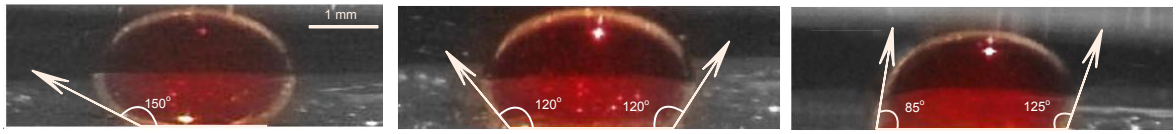

(a) (b) (c)

Figure 5.4: Sequence of droplets showing contact angle variations at different situations. (a) When the manipulation region is under uniform illumination, the droplet contact angle remains unchanged (150°). (b) When the region under the droplet is illuminated by dark light and the remaining active region by bright light, the contact angle reduces at both ends (120°).(c) When a portion of droplet is illuminated by dark light (virtual electrode) and the remaining region by bright light, the contact angle significantly decreases in the end where the dark light is present (85°).

5.1.5 Influence of Virtual Electrode Dimension on Droplet Motion

In OEWOD device, for a specified droplet volume, the droplet movement is externally influenced by the actuation voltage, intensity of the optical source, and the dimension of the virtual electrode. By keeping the actuation voltage (80 V_{DC}) and the optical source (data projector) as constant, the width of the virtual electrode (dark band) is modified to check the droplet behavior. Experiments are conducted by changing the dark band widths by keeping droplet volume as constant and the results are tabulated. Table 5.2 shows the ratio of droplet size and dark band light.

Table 5.2: **Influence of virtual electrode dimension on droplet motion. The table explains the droplet behavior based on the ratio of the droplet volume and virtual electrode dimension. The droplet volume is kept constant (20 μL) and the virtual electrode dimension is varied in each case to check the the droplet behavior.**

Droplet Volume		**Dark Band Width**		**Droplet Radius / Dark Band Width**	**Droplet Behavior**
Volume (μL)	**Radius** (mm)	**Width** (Pixels)	**Width** (mm)		
20	1.75	10	0.9	1.94	No movement
20	1.75	20	1.8	0.97	Continuous droplet movement
20	1.75	25	2.2	0.79	Contact angle changes, no droplet movement
20	1.75	30	2.7	0.65	No movement

Case One: Virtual Electrode width > Droplet Radius

If the virtual electrode width is significantly smaller than the droplet's radius as shown in Figure 5.5(a), only a small portion of droplet region is overlapping the dark band width. Improved wetting is exhibited only on the overlapping droplet region due to optoelectrowetting. so there will not be sufficient reduction in contact angle in the dark band region of droplet and hence there will not be any movement.

Case Two: Virtual Electrode Width $\simeq$ Droplet Radius

If the virtual electrode's width is approximately equal to the droplet's radius as shown in the picture, then half of the droplet will be illuminated by bright light and the other half will be illuminated by the dark region as shown in Figure 5.5(b). The droplet's contact angle under the dark region decreases due to optoelectrowetting and the contact angle of the contact angle in the bright region remains the same. This difference in contact angle at the ends of the droplet helps the droplet moves towards

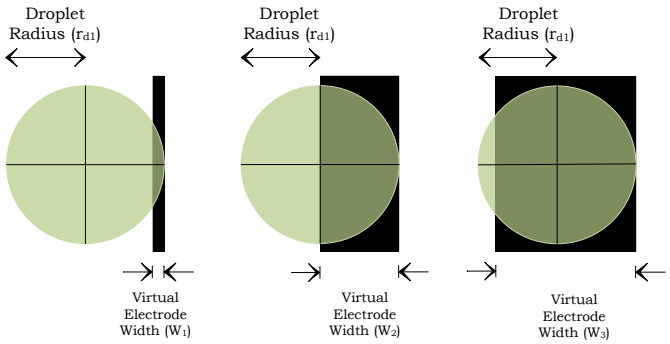

(a) (b) (c)

Figure 5.5: In (a), the droplet radius is significantly larger than the width of the virtual electrode ($r_{d1} > W_1$). In (b), the droplet radius is equal to the width of the virtual electrode ($r_{d1} \approx W_2$). In (c), the droplet radius is significantly smaller than the width of the virtual electrode ($r_{d1} < W_3$).

the wetting direction (towards the virtual electrode).

Case Three: Virtual Electrode Width < Droplet Radius

If the virtual electrode's width is greater than the droplet's radius as shown in Figure 5.5(c), then most of the droplet region will be covered by dark illumination. The droplet contact angle changes at both the ends but the difference in contact angles will be small. Hence no droplet movement is observed.

From the experimental results in Table 5.2, the droplet moves continuously when the virtual electrode width is approximately equal to the droplet radius. The droplet stops moving as the difference between the virtual electrode width and the radius starts increasing. The analysis is verified again using 10 μL droplets as shown in Table 5.3.

5.1.6 Droplet Mixing

Here, merging is tested on both 10 μL and 20 μL droplets. To verify the completion of droplet mixing, we used a 10 μL green droplet (*Fast Green FCF* food dye dissolved in water) and a 10 μL red droplet (*Allura Red AC* food dye dissolved in water) as shown in Figure 5.6. We observed that the merging is instantaneous once the droplets

Table 5.3: Influence of virtual electrode dimension on droplet motion. The table explains the droplet behavior based on the ratio of the droplet volume and virtual electrode dimension. The droplet volume is kept constant (10 μL) and the virtual electrode dimension is varied in each case to check the the droplet behavior.

Droplet Volume		**Dark Band Width**		**Droplet Radius / Dark Band Width**	**Droplet Behavior**
Volume (μL)	**Radius** (mm)	**Width** (Pixels)	**Width** (mm)		
10	1	5	0.45	2.22	No movement
10	1	10	0.90	1.11	Continuous droplet movement
10	1	15	1.35	0.74	Contact angle changes, no droplet movement
10	1	20	1.80	0.56	No movement

comes close to each other. This is because aqueous droplets in oil medium induce electric dipoles. Hence the electrostatic force between two closely located aqueous droplets causes electrocoalescence and merges them [33] [34] [8]. Figure 5.6(c) shows the merged droplet from the red and green droplets but not mixed completely. The upper portion of the merged droplet remains green and the lower portion remains red. The mixing of merged droplet is completed when it is transported to certain distance from its merged location. During transportation, the shear bulk force acting on the moving droplet results in internal flows within the droplet to complete the mixing [8] (Figure 5.6(d)).

5.1.7 Parallel Droplet Movement

The main advantage of optical microfluidics is its ability to transport multiple droplets at the same time. Figures 5.8 and 5.7 show the parallel motion of two droplets at the same time. To verify the performance and ability of the fabricated devices, parallel droplet motion is tested on both the devices A and B. In Device D_{10}, for 120 V_{DC} input, two droplets (20 μL each) are simultaneously transported at approximately 3 mm/sec. In Device D_{25}, for the same voltage and same volume, two

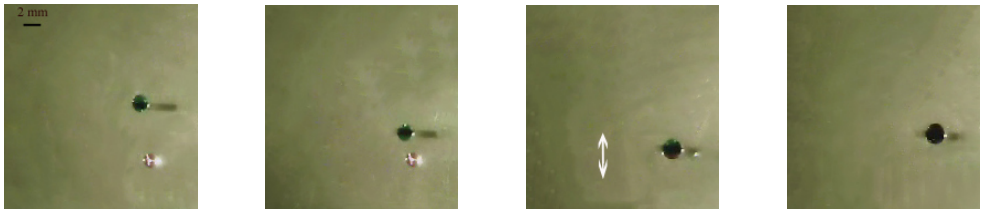

(a) (b) (c) (d)

Figure 5.6: Sequence of Droplet Mixing. (a) The initial position of two colored (green and red) droplets (10 μL). (b) The green droplet has moved towards the red droplet which is kept stationary in its initial position. (c) Once the red and green droplets are merged, the upper portion of the merged droplet remains green and the lower portion remains red. (d) The mixed droplet after it has been moved in both the directions.

droplets were simultaneously transported at approximately 7.3 mm/sec. We observed that the input voltage and average velocity of droplet movement remains the same for individual and parallel operations for a device. The velocity of individual droplets are not reduced by increasing the total number of droplets in parallel operation. This ability to actuate droplets in parallel at equal voltage and velocities can potentially play a key role in miniaturizing cell culture microplates for biological applications.

(a) (b) (c)

Figure 5.7: Sequence of parallel motion in device D_{10}. Two droplets are transported simultaneously by virtual electrodes moving at 3 mm/sec.

5.1.8 Droplet manipulation multiple axis

This OEWOD device is capable of transporting droplets in multi-direction at low voltage actuation and high droplet velocity. Previous reported open configuration devices reported difficulties in multiaxis motion. [28] reported that the droplets

(a) (b) (c)

Figure 5.8: Sequence of parallel motion in device D_{25}. Two droplets are transported simultaneously by virtual electrodes moving at 7 mm/sec.

transportation is difficult due to weak electric field strength in the direction perpendicular to the applied electric field. Optical patterns of different shapes are used (Paired-Diamond (PD)) to increase the electric field strength in both the directions for achieving multi-axis droplet motion [9]. Still, the droplet actuation voltage is very high (300 V_{DC}) and the droplet velocity is very low ($\simeq$ 500 μ m/sec). In our OEWOD device, we achieved low voltage multi-axis motion by enhancing the electric field strength in both the directions without modifying the shapes of optical pattern. The electric field strength is enhanced by fabricating gold contact pads surrounding the active region (Figure **??**).

To experimentally verify the multi-axis motion, we transported a droplet in two different axis (at same voltage and velocity) using two different virtual electrodes of same dimension. The first virtual electrode is oriented along the vertical axis and the second virtual electrode along the horizontal axis as shown in Figure 5.9(a). A green droplet (10 μL) is introduced on the device surface. By applying voltage (85 V_{DC}) at contact pad set CP_y, the first virtual electrode transports the droplet from position X to position Y (Figure 5.9 (a) & (b)). Subsequently, the second virtual electrode transports the same green droplet from position Y to position Z (Figure 5.9 (c) & (d)) by applying the same voltage at contact pad set CP_x.

The only limitation is that these experiments are conducted by manually applying voltage at contact pad sets CP_x and CP_y shown in Figure 5.2. At a given instant,

only one set of contact pad will be connected with the external voltage. To avoid time delay and human interference, future experiments will be conducted by applying external voltage using digital timer switch between contact pad sets. These digital timer switches can be from timers and software switches used in microcontrollers. By using these timer switches, the external voltage can be switched between CP_x to CP_y within millisecond time delay.

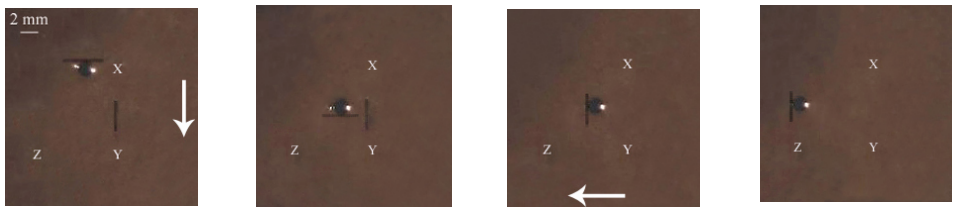

(a) (b) (c) (d)

Figure 5.9: The sequence shows multi-axis motion in OEWOD device. CP_1 and CP_2 represent the sides of the contact pads. (a) The green droplet (10 μL) is in its initial position X. (b) The first virtual electrode transports the droplet from position X to position Y while the second virtual electrode is kept stationary. (c) The first virtual electrode is turned off, and the second virtual electrode starts transporting the droplet from position Y to position Z. (d) The final position of the droplet.

5.2 Contributions

In this research, we reported an open surface light-actuated optoelectrowetting microfluidic device that can manipulate droplets of multiple volumes ranging from 1 to 50 μL at voltage as low as 53 V_{DC} and capable of transporting droplets at a maximum speed of 12 mm/sec (120 V_{DC}). We achieved this low voltage activation by adding a dedicated Al_2O_3 dielectric layer of high dielectric constant and significantly reducing the thickness of the hydrophobic layer. The advantages of this device are the low voltage droplet actuation, high speed droplet manipulation, and multi-axis parallel droplet motion. This device can perform basic DMFS operations like transportation, mixing, and merging at low voltage and we demonstrated multiple axis parallel droplet motion at equal velocities in all directions without modifying the optical patterns. We

also reported the behavioral changes in droplet actuation influenced by the optical pattern dimensions and its relation with the droplet volume.

5.3 Future work

In this research, the performance of OEWOD device is improved by reducing the voltage required for droplet manipulation. The threshold voltage can be further reduced by increasing the dielectric constant of the hydrophobic layer. The compact voltage sources like AA lithium batteries can be used, if the threshold voltage required is less than 10 V. Miniaturization of the voltage source (6 V, AA lithium battery) will be critical in achieving device portability. The significant reduction in droplet actuation voltage along with the enhanced capability of low voltage multi-axis manipulation using this OEWOD device is a step towards achieving a portable light-actuated digital microfluidic device.

BIBLIOGRAPHY

[1] D. Figeys and D. Pinto, "Lab-on-a-chip: A revolution in biological and medical sciences.," *Analytical Chemistry*, vol. 72, no. 9, pp. 330 A–335 A, 2000.

[2] H. P. Le, "Progress and trends in ink-jet printing technology," *The Journal of Imaging Science and Technology*, vol. 42, pp. 49–62, Jan. 1998.

[3] S. Haeberle and R. Zengerle, "Microfluidic platforms for lab-on-a-chip applications," *Lab Chip*, vol. 7, pp. 1094–1110, 2007.

[4] S. Terry, J. Jerman, and J. Angell, "A gas chromatographic air analyzer fabricated on a silicon wafer," *Electron Devices, IEEE Transactions on*, vol. 26, pp. 1880 – 1886, Dec. 1979.

[5] S. Shoji, M. Esashi, and T. Matsuo, "Prototype miniature blood gas analyser fabricated on a silicon wafer," *Sensors and Actuators*, vol. 14, no. 2, pp. 101 – 107, 1988.

[6] H. van Lintel, F. van De Pol, and S. Bouwstra, "A piezoelectric micropump based on micromachining of silicon," *Sensors and Actuators*, vol. 15, no. 2, pp. 153 – 167, 1988.

[7] P. Y. Chiou, H. Moon, H. Toshiyoshi, C. J. Kim, and M. C. Wu, "Light actuation of liquid by optoelectrowetting," *Sensors and Actuators A: Physical*, vol. 104, no. 3, pp. 222 – 228, 2003.

[8] S. Y. Park, M. A. Teitell, and E. P. Y. Chiou, "Single-sided continuous optoelectrowetting (SCOEW) for droplet manipulation with light patterns," *Lab Chip*, vol. 10, pp. 1655–1661, 2010.

[9] S.-Y. Park, S. Kalim, C. Callahan, M. A. Teitell, and E. P. Y. Chiou, "A light-induced dielectrophoretic droplet manipulation platform," *Lab Chip*, vol. 9, no. 22, pp. 3228–3235, 2009.

[10] S.-Y. Park and P.-Y. Chiou, "Light-driven droplet manipulation technologies for lab-on-a-chip applications," *Advances in OptoElectronics*, vol. 2011, p. 12, Aug. 2011.

[11] M. W. L. Watson, M. Abdelgawad, G. Ye, N. Yonson, J. Trottier, and A. R. Wheeler, "Microcontact printing-based fabrication of digital microfluidic devices," *Analytical Chemistry*, vol. 78, no. 22, pp. 7877–7885, 2006.

[12] M. G. Pollack, R. B. Fair, and A. D. Shenderov, "Electrowetting-based actuation of liquid droplets for microfluidic applications," *Applied Physics Letters*, vol. 77, pp. 1725 –1726, sep. 2000.

[13] C.-J. Kim, H. Moon, S. K. Cho, and R. L. Garrell, "Low voltage electrowetting-on-dielectric," *Journal of Applied Physics*, vol. 92, pp. 4080–4087, Oct. 2002.

[14] C. Quilliet and B. Berge, "Electrowetting: a recent outbreak," *Current Opinion in Colloid and amp; Interface Science*, vol. 6, no. 1, pp. 34 – 39, 2001.

[15] M. G. Pollack, A. D. Shenderov, and R. B. Fair, "Electrowetting-based actuation of droplets for integrated microfluidics," *Lab Chip*, vol. 2, pp. 96–101, 2002.

[16] Y. Li, W. Parkes, L. Haworth, A. Ross, J. Stevenson, and A. Walton, "Room-temperature fabrication of anodic tantalum pentoxide for low-voltage electrowetting on dielectric (ewod)," *Microelectromechanical Systems, Journal of*, vol. 17, pp. 1481 –1488, dec. 2008.

[17] W. Gonzalez-Vinas and H. L. Mancini, *An Introduction to Material Science*. Princeton university press, 2004.

[18] Y.-Y. Lin, R. D. Evans, E. Welch, B.-N. Hsu, A. C. Madison, and R. B. Fair, "Low voltage electrowetting-on-dielectric platform using multi-layer insulators," *Sensors and Actuators B: Chemical*, vol. 150, no. 1, pp. 465–470, 2010.

[19] R. Fair, V. Srinivasan, H. Ren, P. Paik, V. Pamula, and M. Pollack, "Electrowetting-based on-chip sample processing for integrated microfluidics," in *Electron Devices Meeting, 2003. IEDM '03 Technical Digest. IEEE International*, pp. 32.5.1 – 32.5.4, Dec. 2003.

[20] B. S. Gallardo, V. K. Gupta, F. D. Eagerton, L. I. Jong, V. S. Craig, R. R. Shah, and N. L. Abbott, "Electrochemical principles for active control of liquids on submillimeter scales," *Science*, vol. 283, no. 5398, pp. 57–60, 1999.

[21] T. S. Sammarco and M. A. Burns, "Thermocapillary pumping of discrete drops in microfabricated analysis devices," *AIChE Journal*, vol. 45, no. 2, pp. 350–366, 1999.

[22] T. B. Jones, M. Gunji, M. Washizu, and M. J. Feldman, "Dielectrophoretic liquid actuation and nanodroplet formation," *Journal of Applied Physics*, vol. 89, no. 2, pp. 1441–1448, 2001.

[23] A. Ashkin and J. M. Dziedzic, "Optical levitation of liquid drops by radiation pressure," *Science*, vol. 187, no. 4181, pp. 1073–1075, 1975.

[24] N. Magome, M. I. Kohira, E. Hayata, S. Mukai, and K. Yoshikawa, "Optical trapping of a growing water droplet in air," *The Journal of Physical Chemistry B*, vol. 107, no. 16, pp. 3988–3990, 2003.

[25] B. Selva, V. Miralles, I. Cantat, and M.-C. Jullien, "Thermocapillary actuation by optimized resistor pattern: bubbles and droplets displacing, switching and trapping," *Lab Chip*, vol. 10, pp. 1835–1840, 2010.

[26] A. A. Darhuber, J. P. Valentino, J. M. Davis, S. M. Troian, and S. Wagner, "Microfluidic actuation by modulation of surface stresses," *Applied Physics Letters*, vol. 82, no. 4, pp. 657–659, 2003.

[27] P. Y. Chiou, S. Y. Park, and M. C. Wu, "Continuous optoelectrowetting for picoliter droplet manipulation," *Applied Physics Letters*, vol. 93, pp. 221110 – 221110–3, Dec. 2008.

[28] S. Park, C. Pan, T.-H. Wu, C. Kloss, S. Kalim, C. E. Callahan, M. Teitell, and E. P. Y. Chiou, "Floating electrode optoelectronic tweezers: Light-driven dielectrophoretic droplet manipulation in electrically insulating oil medium," *Journal of Applied Physics*, vol. 92, no. 15, pp. 151101(1) – 151101(3), 2008.

[29] S. N. Pei, J. Valley, S. Neale, A. Jamshidi, H.-Y. Hsu, and M. Wu, "Light-actuated digital microfluidics for large-scale, parallel manipulation of arbitrarily sized droplets," in *Micro Electro Mechanical Systems (MEMS), 2010 IEEE 23rd International Conference*, pp. 252 –255, Jan. 2010.

[30] J. Berthier, *Microdrops and digital microfluidics*. Micro & nano technologies, William Andrew Pub., 2008.

[31] K. E. Herold and A. Rasooly, *Lab-on-a-Chip Technology: Fabrication and Microfluidics*, vol. 1. Caister Academic Press, 1 ed., Aug. 2009.

[32] J. R. Millman, K. H. Bhatt, B. G. Prevo, and O. D. Velev, "Anisotropic particle synthesis in dielectrophoretically controlled microdroplet reactors.," *Nature Materials*, vol. 4, no. 1, pp. 98–102, 2005.

[33] C. Priest, S. Herminghaus, and R. Seemann, "Controlled electrocoalescence in microfluidics: Targeting a single lamella," *Applied Physics Letters*, vol. 89, no. 13, pp. 134101(1)–134101(3), 2006.

[34] M. Zagnoni and J. M. Cooper, "On-chip electrocoalescence of microdroplets as a function of voltage, frequency and droplet size," *Lab Chip*, vol. 9, no. 18, pp. 2652–2658, 2009.